

One Picture is Worth a Thousand Words: A New Wallet Recovery Process

Hervé Chabanne
IDEMIA and Télécom Paris
herve.chabanne@telecom-paris.fr

Vincent Despiegel
IDEMIA

Linda Guiga
IDEMIA and Télécom Paris

Abstract—We introduce a new wallet recovery process. Our solution associates 1) visual passwords: a photograph of a secretly picked object (Chabanne et al., 2013) with 2) ImageNet classifiers transforming images into binary vectors and, 3) obfuscated fuzzy matching (Galbraith and Zobernig, 2019) for the storage of visual passwords/retrieval of wallet seeds. Our experiments show that the replacement of long seed phrases by a photograph is possible.

Index Terms—Cryptographic Obfuscation, Imagenet Classifier, Application of Machine Learning to Cryptocurrency Wallets

I. INTRODUCTION

Cryptocurrency wallets store private keys and make use of them for performing transactions among blockchains. Their loss is identified in [14] as one of the three challenges associated to Bitcoin. Today, they mainly rely on a seed phrase for their recovery [26]. In 2021, the New York Times reported [1] that “20 percent of the existing 18.5 million Bitcoin or around 3.7 million BTCs appear to be lost due to forgotten passwords”.

To alleviate the burden of remembering this long password, we alternatively rely on the concept of visual passwords introduced in 2013 by Chabanne et al. [11].

The underlying principle of visual passwords is, in the context of authentication, the following:

- At the registration step, you choose an object and take a photograph of it. Your choice has to remain secret.
- When you want to authenticate yourself, you take another photograph of the same object for a comparison image vs image with the reference.

While [11] focuses on a single type of object: Hamiltonian circuits among a cube, with a design enabling many possible configurations; to ensure a good entropy, we here let the users choose among a great variety of different objects.

A special care is taken to the storage of references. We apply the work of Galbraith and Zobernig [17] to perform Hamming ball membership determining in an obfuscated way whether a binary vector lies close to a predetermined center.

Our main contribution is the introduction of a novel wallet recovery system. Moreover, we show its feasibility

by our experiments transforming visual passwords by state of the art image processing algorithms into suitable binary vectors, called *templates* in the following, for secure storage/ seed retrieval.

The rest of the paper is organized as follows: in Sec. II we recall the techniques and security properties of obfuscated Hamming distance comparisons and show how to deliver a payload in case of a matching. In Sec. III, we describe how to transform visual password pictures into binary vector templates thanks to deep learning algorithms. In Sec. IV, we report our experiments. Sec. V details our proposal. Sec. VI concludes.

A. Related Works

For a general introduction to wallets in the context of Bitcoin; see, for instance, chapter 4 of [23].

While there are numerous other attempts to replace passwords using graphical interfaces and images [8], visual passwords [11] share a lot with biometric recognition. For instance, we are using in Sec. IV the same tools to evaluate the accuracy of our proposal, namely:

- The *False Acceptance Rate* (FAR) measures the proportion of times an imposter can fool the system. FAR is directly related to the security level.
- On the opposite, the user’s convenience is gauged thanks to the *False Reject Rate* (FRR) which corresponds to genuine attempts dismissed.

As one cannot win both at the same time with FAR and FRR, the *Detection Error Tradeoff* (DET) curve which represents false rejection rate vs. false acceptance rate comes into consideration for determining the *Equal Error Rate* (EER) of the system where FAR and FRR are equal.

Major differences however differentiate biometrics and visual passwords. Biometrics are public and immutably linked to a person while visual passwords are secret and easy to renew. For instance, biometrics need liveness anti-spoofing countermeasures to thwart impersonation attacks and depending on their application, privacy enhancing technologies are necessary too.

Fuzzy matching has already been considered in the context of biometrics, around the notion of *secure sketch* introduced in [15]. Here the matching is realized thanks to an underlying error correcting code. As indicated in [17], parameters of secure sketch are thus “strongly constrained

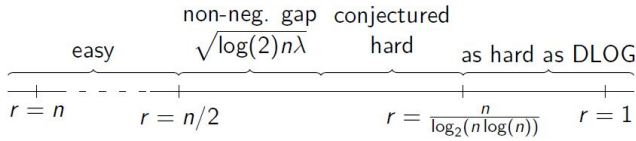


Fig. 1: Hardness of MSP Problem

by the need for an efficient decoding algorithm”. Moreover, when it comes to their implementation with real (biometric) data, their security is questionable [29], in particular regarding their reusability.

Cryptographic techniques such as a secret sharing mechanism [22] or multi-signature techniques [19] can also be envisaged for cryptocurrency wallets. Our proposal is – the same way, that passphrases are – complementary. Another solution [27] relies on a Diffie-Hellman exchange between hardware wallets with a human visual verification to thwart man-in-the-middle attacks.

II. OBFUSCATED FUZZY HAMMING DISTANCE MATCHING

In this section, we show how to store our reference binary vector templates in a way that enables Hamming distance comparisons while preserving their confidentiality. I.e. we retrieve the wallet’s seed when and only when a fresh template close to the reference is entered. For that, we make use of cryptographic obfuscation.

Obfuscation makes programs unintelligible while preserving their functionality. General obfuscation techniques are either impossible [7] or, despite major progress [21], ineffective. In 2014, [6] defines practical input-hiding obfuscation techniques for evasive functions including *point functions* “ $x == e$ ”, which return 1 when the input is equal to a predetermined constant e and 0 otherwise.

Example 1: [34] describes how to obfuscate variable comparisons “ $ax + b == y$ ” where a, b are two k -bits constants. Let H stand for a preimage-resistant hash function with n -bits outputs, $n > k$. Choose at random $t \in \{0, 1\}^{n-k}$ and $r \in \{0, 1\}^k$. Let $h = H(r||t)$ and $u = r + b$. Values a, u, h are published. The obfuscated program then checks

$$H(ax + u - y||t) == h \quad (1)$$

while keeping the value b hidden. Note that when (1) is verified by inputs (x, y) , b can be retrieved as $b = y - ax$.

Relying on a number-theoretic computational assumption called the Modular Subset Product (MSP) problem (see Fig. 1), [17] defines a Hamming distance obfuscator which checks whether an n -bits binary vector x is within Hamming distance r of a predetermined c for

$$r \leq n/2 - \sqrt{\log(2)n\lambda} \quad (2)$$

where λ is a security parameter.

A vector $c = (c_1, \dots, c_n) \in \{0, 1\}^n$ is encoded as

$$\text{ENCODE}(c) = ((p_i)_{i=1, \dots, n}, q, C) \quad (3)$$

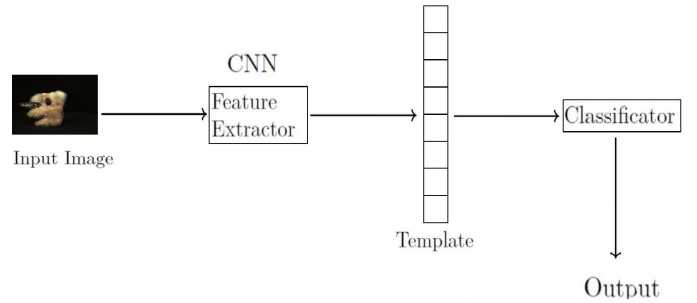


Fig. 2: An ImageNet Classifier

where

- $C = \prod_{i=1}^n p_i^{c_i} \bmod q$;
- $(p_i)_{i=1, \dots, n}$ are small distinct primes taken at random for each encoding;
- q is a small safe prime verifying $\prod_{i \in I} p_i < q/2$ for all $I \subset \{1, \dots, n\}$ with cardinality $|I| < r$. Typically, $q \sim (n \log n)^r$.

This encoding procedure keeps the vector c hidden when

$$r > \log(2\sqrt{2\pi e}) \frac{n}{\log(n \log(n))} \quad (4)$$

A procedure DECODE is then defined s.t. $\text{DECODE}((p_i)_{i=1, \dots, n}, q, C, x) = c$ for each vector x which stands at Hamming distance $d(c, x) < r$. This procedure returns \perp for x s.t. $d(c, x) \geq r$ except when a false acceptance occurs. Note that, when r satisfies (4), this false acceptance cannot happen, see Sec. IV-C and [17] for details.

The obfuscated program with embedded data $(p_i)_{i=1, \dots, n}, q, C$ is executed as follows for an input x :

$\mathbf{1}_1$: $c' = \text{DECODE}((p_i)_{i=1, \dots, n}, q, C, x)$

$\mathbf{1}_2$: If $c' = \perp$ Return 0

$\mathbf{1}_3$: Return the obfuscated point function comparison to c

In [17], the last line $\mathbf{1}_3$ eliminates false acceptances. Write now $c = c_1 || c_2$ and for b at random, $ac_1 + b = c_2$. In our proposal, we replace $\mathbf{1}_3$ by (using the notations introduced in Example 1):

$\mathbf{1}_3'$: If (1) stands for inputs $c'_1 || c'_2 = c'$ Return $b = c'_2 - ac'_1$; else Return \perp

We then obtain the RETRIEVESEED program comprised of the three lines: $\mathbf{1}_1, \mathbf{1}_2, \mathbf{1}_3'$.

III. PICTURES PROCESSING

In this section, we describe our choices for transforming photographs of visual passwords into binary vector templates. Our experiments are reported in the next section.

A. Templates Construction

Consider the architecture of an ImageNet classifier as in Fig. 2. It takes as an input an image from which its features are extracted thanks to a Convolutional Neural



Fig. 3: Different Views of Object 197

Network (CNN) to eventually output a classification. Similarly to the idea used in Face Recognition algorithms, the underlying representation is a good candidate feature for object recognition even if the objects were not in the training dataset. Consequently, in a first step, we remove the last classification layers to just keep floating point vectors of the internal representation. Finally, we binarize these vectors to obtain our templates.

B. Model Choice

We choose a model trained (with its parameters) among <https://paperswithcode.com/sota/image-classification-on-imagenet>.

After different trials (see Annex A), we pick VGG-16 [30] as the underlying model to classify images. This leads to vectors with 4096 floating-point coordinates. To reduce the dimension to only 512 bits, we apply Locality Sensitive Hashing (LSH) [20]. For this, we generate a random sparse matrix of shape $(4096, 512)$ thanks to the Scikit library: <https://scikit-learn.org/stable/>. We then multiply the generated matrix by the original coordinates. Lastly, we only keep the signs of the resulting vector elements so as to turn the floating values into binary ones. At the end, our overall architecture is similar to the perceptual hashing algorithm NeuralHash [2].

IV. EXPERIMENTS

A. Test Dataset

To validate our experiments, we use the Amsterdam Library of Object Images (ALOI) [18]. The ALOI dataset is made of 1,000 objects recorded under various viewing angles, illumination angles, and illumination colors (Fig. 3), yielding a total of 110,250 images for the collection.

B. Accuracy

To test the accuracy of our system, we select, for each object, 3 different views – corresponding to rotation angles of 0, 15 and 35 degrees – which seems realistic in terms of noise for the target scenario. We then obtain the resulting DET curves shown in Fig. 4.

From our observations, our binarization process only slightly degrades our overall accuracy. Some more sophisticated methods as in [32] could be used for binarization but as the degradation is under control, our experiments stick to this simple method.

C. Implementation Details

With $n = 512$, we choose $r = 140$, placing ourselves at the rightmost part of Fig. 1. These parameters satisfy both inequalities (2) and (4).

Our implementation of the ENCODE (resp. RETRIEVESEED) procedure yields on our laptop an average encoding time (resp. decoding time) of 50 ms (resp. 10 ms). These timings are in line with the ones given by [17].

We obtain then an FAR around 4.10^{-4} for a rotation angle of 15 degrees (resp. 35 degrees) and a corresponding FRR of 1.8% (resp. 7%). Note that, in our system – in opposition to biometric systems where a false reject can imply for a user to be blocked at a gate – a false reject simply demands for a new photograph of the referenced object to be taken.

Remark 1: A user can store different objects. For each of them, its encoding enables us to hide a new secret k_i , $i = 1, \dots, m$. By taking the exclusive OR of all of them $k_1 \oplus \dots \oplus k_m = k$, the resulting k is obtained for an illegitimate user when and only when each of the m objects he had chosen leads to an encoding which matches with the genuine stored object.

V. OUR PROPOSAL

As pointed out by [5], there is a huge gap, e.g. for VGG-16, regarding the intrinsic dimension – i.e. the minimal number of parameters needed to describe a representation – between input images and outputs of CNNs. We rely on that observation to mitigate the risk of an attack which looks for false positives.

We thus envisage to implement a proprietary algorithm on a dedicated server – i.e. with dedicated metaparameters and training – to compute templates corresponding to photos of objects. This way, template requests can be recorded and a security policy be established to limit their number, enforcing access control to templates.

To protect users against the server, we suggest sending visual passwords encrypted thanks to homomorphic encryption. Template computation is now possible directly in the encrypted domain [13] and new progress is announced [9], [28].

We now consider that a homomorphic encryption scheme is chosen [4] and that users generate their own private key for this scheme. Note that they do not have to keep them.

A. Detailed Description

Our system is made of:

- users;
- a dedicated server S in charge of computing templates for users from their visual password.

The different steps of our wallet recovery process are summarized in Fig. 5

More specifically, a user U is going to ENCODE his template (3) and perform RETRIEVESEED using his own device; e.g. his mobile phone. This device also enables him

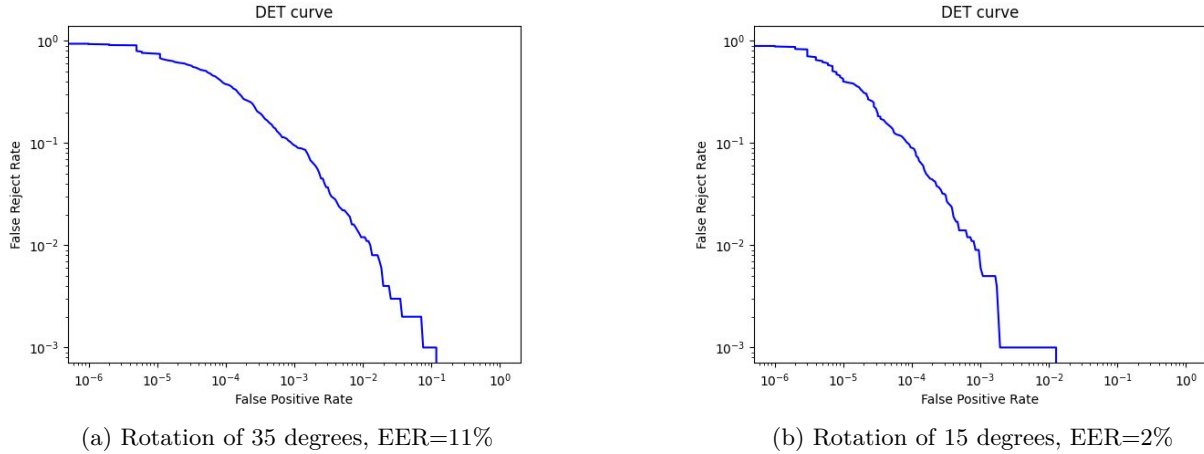


Fig. 4: DET Curves

Setup:

- User U picks his visual password
- U generates his key for the underlying homomorphic encryption scheme and encrypts his visual password
- U asks the dedicated server S for the template associated to his visual password
- S computes U 's template, c , encrypted
- U decrypts c , computes $\text{ENCODE}(c)$ (3) and stores it at a place of his choice

Seed Recovery:

- U gets back $\text{ENCODE}(c)$ and takes a new photograph of his visual password, (optionally, if needed, U generates a new homomorphic encryption key), encrypts it and sends the ciphertext to S
- U asks S for the template x corresponding to this new photograph
- S computes x in an encrypted form
- U decrypts x and retrieves his wallet's seed as $\text{RETRIEVESEED}(\text{ENCODE}(c), x)$

Fig. 5: Our Wallet Recovery Process

to capture and then, encrypt his visual password (resp. decrypt his template) before sending it to S (resp. after receiving it from S). We consider that all these operations performed on the device of U are safe from attacks.

The way his wallet's seed is used after its retrieval is out-of-scope of this paper.

Server S is considered honest-but-curious regarding the requests from the users. It protects the implementation of the proprietary model M and restricts templates computation.

B. Security Discussion

We consider three factors to be taken into account for the security of our wallet seeds recovery process:

- Storage of the obfuscated template;
- Access to a templates construction algorithm;
- Choice diversity for visual passwords.

Our threat model is simple: we want to protect against an adversary who tries to retrieve the wallet's seed by presenting a binary vector close to the stored reference template.

Having access to the know-how for transforming visual passwords into templates enables this adversary to attempt to obtain a false acceptance. Otherwise, we rely on the security provided by the obfuscated fuzzy Hamming distance matching. Searching in $\{0, 1\}^n$, $n = 512$ leads to a probability of $1/2^\lambda$ with $\lambda = 87$ for $r = 140$ (see (2)) to find by chance a vector in the targeted Hamming ball. In contrast, the knowledge of the underlying templates subspace enables the adversary to drastically reduce his efforts with a FAR of 4.10^{-4} (see also Annex B). The confidentiality of the model M is paramount for our wallet recovery process.

Regarding that point, besides server compromise, given oracle access to a neural network as in our proposal, model extraction attacks can be launched [31]. Today, the best attacks [10], [12], [24], [25], [33] against ImageNet classifiers seem unpractical. Note also that a first defense strategy keeping the model's accuracy has been introduced in [16].



Fig. 6: Objects 196, 197, 198 side-by-side

VI. CONCLUSION

We are confident that there is room for improvement of the accuracy of our system. For instance, facial recognition which is an image processing problem of roughly the same difficulty as ours obtains less than 1% of FRR at FAR of 10^{-6} with systems working all around the world [3]. Our performances of Sec. IV-B look poor in comparison. As usual in big data, a huge dataset might enable us to improve our model. We are currently looking for a larger database of objects to work with. For instance, regarding the FAR we obtained, the presence of various objects which look similar – see, for instance, Fig. 6 – among the 1,000 within ALOI, tends to increase this rate in our experiments. A user does have a much larger choice at his disposal. For instance, a museum collection often counts more than a million objects while offering a long term storage for them.

APPENDIX A SELECTED MODEL

To turn images into binary vectors, we use an NN. We opt for the VGG architecture after various trials. For instance, we tried the pretrained EfficientNet architecture, which has a higher accuracy on ImageNet (see <https://paperswithcode.com/sota/image-classification-on-imagenet>). However, it yields a higher FRR for a given FAR on ALOI, as can be seen in Fig. 7.

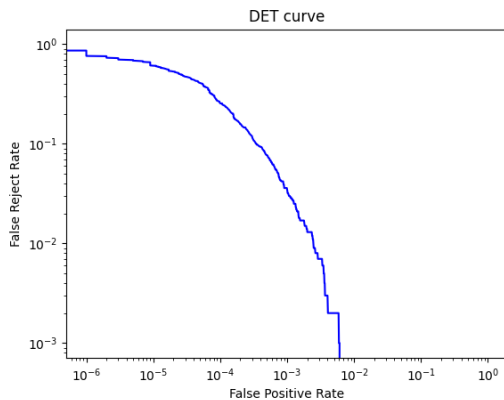


Fig. 7: Rotation of 15 degrees on EfficientNet.

Similarly, in order to reduce the number of bits from 4,096 to 512, we select LSH even though other methods, such as Principal Component Analysis (PCA) exist. However, PCA depends on the training data, when LSH is

independent of it. If the PCA is determined on Imagenette data rather than ALOI images, the resulting accuracy is lower than LSH, as can be seen in Fig. 8.

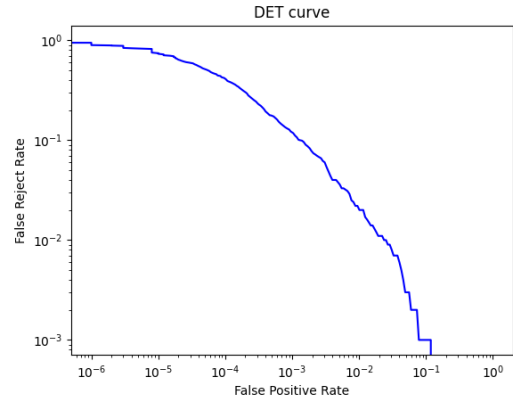


Fig. 8: Rotation of 15 degrees with PCA on VGG-16.

APPENDIX B PROBABILITY OF RANDOMLY SELECTING A TEMPLATE IN THE HAMMING BALL

[17] determines an upper bound for the probability of randomly selecting an element $y \in \{0,1\}^n$ in $B_x(r)$, the Hamming ball of radius r and center x , taking also into account a security parameter λ .

In our case, for $n = 512$, $r = 140$ and $\lambda = 87$, we have: $Pr_{y \in \{0,1\}^{512}}[y \in \mathcal{B}_x(140)] \leq \frac{1}{2^{87}}$.

Exploiting the inherent correlation between coordinates of templates, we are now going to estimate an upper bound for

$$Pr_{y \in \{0,1\}^n \cap \text{Templates subspace}}[y \in \mathcal{B}_x(r)]$$

corresponding to when an adversary restricts himself to search among the templates subspace. This is the case when he has access to the model M .

Moreover in our experiments, we restrict ourselves to image inputs and we compute the templates of the 13,394 images coming from the Imagenette dataset (<https://github.com/fastai/imagenette>) searching for a false acceptance with one of the 1,000 templates of the ALOI dataset (without any rotation). We obtain that 4 among these 1,000 ALOI templates get a false acceptance – a distance less than 140 – with respectively 2, 12, 1 and 2 templates coming from the other dataset. This leads to a ratio of 1.27×10^{-6} of the comparisons. We lose two orders of magnitude from the FAR of Sec. IV-C due to the fact that we are here looking at images that can be quite quite different than the objects from ALOI.

ACKNOWLEDGEMENTS.

This work was partly supported by the iMARS project (G.A. no 883356), funded by the European Union’s Horizon 2020 research and innovation program.

REFERENCES

- [1] <https://www.nytimes.com/2021/01/13/business/tens-of-billions-worth-of-bitcoin-have-been-locked-by-people-who-forgot-their-key.html>.
- [2] <https://github.com/AsuharietYgvar/AppleNeuralHash2ONNX>.
- [3] https://pages.nist.gov/frvt/reports/11/frvt_11_report.pdf.
- [4] Martin Albrecht, Melissa Chase, Hao Chen, Jintai Ding, Shafi Goldwasser, Sergey Gorbunov, Shai Halevi, Jeffrey Hoffstein, Kim Laine, Kristin Lauter, Satya Lokam, Daniele Micciancio, Dustin Moody, Travis Morrison, Amit Sahai, and Vinod Vaikuntanathan. Homomorphic encryption security standard. Technical report, HomomorphicEncryption.org, 2018.
- [5] Alessio Ansuini, Alessandro Laio, Jakob H. Macke, and Davide Zoccolan. Intrinsic dimension of data representations in deep neural networks. In *NeurIPS*, pages 6109–6119, 2019.
- [6] Boaz Barak, Nir Bitansky, Ran Canetti, Yael Tauman Kalai, Omer Paneth, and Amit Sahai. Obfuscation for evasive functions. In *TCC*, volume 8349 of *Lecture Notes in Computer Science*, pages 26–51. Springer, 2014.
- [7] Boaz Barak, Oded Goldreich, Russell Impagliazzo, Steven Rudich, Amit Sahai, Salil P. Vadhan, and Ke Yang. On the (im)possibility of obfuscating programs. In *CRYPTO*, volume 2139 of *Lecture Notes in Computer Science*, pages 1–18. Springer, 2001.
- [8] Robert Biddle, Sonia Chiasson, and Paul C. van Oorschot. Graphical passwords: Learning from the first twelve years. *ACM Comput. Surv.*, 44(4):19:1–19:41, 2012.
- [9] Charlotte Bonte, Rosario Cammarota, Wei Dai, Joshua Fryman, Huijing Gong, Duhyeong Kim, Raghavan Kumar, Poornima Lalwaney Kim Laine, Sanu Mathew, Nojan Sheybani, Anand Rajan, Andrew Reinders, Michael Steiner, Vikram Suresh, Sachin Taneja, Marc Trifan, Alexander Viand, Wei Wang, Wen Wang, Chris Wilkerson, and Jin Yang. Is revolutionary hardware for fully homomorphic encryption important? What else is needed? *COSADE*, 2021.
- [10] Nicholas Carlini, Matthew Jagielski, and Ilya Mironov. Cryptanalytic extraction of neural network models. In *CRYPTO (3)*, volume 12172 of *Lecture Notes in Computer Science*, pages 189–218. Springer, 2020.
- [11] Hervé Chabanne, Jean-Michel Cioranescu, Vincent Despiegel, Jean-Christophe Fondeur, and David Naccache. Using hamiltonian totems as passwords. *IACR Cryptol. ePrint Arch.*, page 751, 2013.
- [12] Varun Chandrasekaran, Kamalika Chaudhuri, Irene Giacomelli, Somesh Jha, and Songbai Yan. Exploring connections between active learning and model extraction. In *USENIX Security Symposium*, pages 1309–1326. USENIX Association, 2020.
- [13] Ilaria Chillotti, Marc Joye, and Pascal Paillier. Programmable bootstrapping enables efficient homomorphic inference of deep neural networks. In *CSCML*, volume 12716 of *Lecture Notes in Computer Science*, pages 1–19. Springer, 2021.
- [14] Mauro Conti, Sandeep Kumar E, Chhagan Lal, and Sushmita Ruj. A survey on security and privacy issues of bitcoin. *IEEE Commun. Surv. Tutorials*, 20(4):3416–3452, 2018.
- [15] Yevgeniy Dodis, Leonid Reyzin, and Adam D. Smith. Fuzzy extractors: How to generate strong keys from biometrics and other noisy data. In *EUROCRYPT*, volume 3027 of *Lecture Notes in Computer Science*, pages 523–540. Springer, 2004.
- [16] Adam Dziedzic, Muhammad Ahmad Kaleem, Yu Shen Lu, and Nicolas Papernot. Increasing the cost of model extraction with calibrated proof of work. *CoRR*, abs/2201.09243, 2022.
- [17] Steven D. Galbraith and Lukas Zobernig. Obfuscated fuzzy hamming distance and conjunctions from subset product problems. In *TCC (1)*, volume 11891 of *Lecture Notes in Computer Science*, pages 81–110. Springer, 2019.
- [18] Jan-Mark Geusebroek, Gertjan J. Burghouts, and Arnold W. M. Smeulders. The Amsterdam Library of Object Images. *Int. J. Comput. Vis.*, 61(1):103–112, 2005. URL: <https://aloi.science.uva.nl/>.
- [19] Jongbeen Han, Mansub Song, Hyeonsang Eom, and Yongseok Son. An efficient multi-signature wallet in blockchain using bloom filter. In *SAC*, pages 273–281. ACM, 2021.
- [20] Piotr Indyk and Rajeev Motwani. Approximate nearest neighbors: Towards removing the curse of dimensionality. In *STOC*, pages 604–613. ACM, 1998.
- [21] Aayush Jain, Huijia Lin, and Amit Sahai. Indistinguishability obfuscation from well-founded assumptions. In *STOC*, pages 60–73. ACM, 2021.
- [22] Stanislaw Jarecki, Aggelos Kiayias, Hugo Krawczyk, and Jiayu Xu. Highly-efficient and composable password-protected secret sharing (or: How to protect your bitcoin wallet online). In *EuroS&P*, pages 276–291. IEEE, 2016.
- [23] Arvind Narayanan, Joseph Bonneau, Edward W. Felten, Andrew Miller, and Steven Goldfeder. *Bitcoin and Cryptocurrency Technologies - A Comprehensive Introduction*. Princeton University Press, 2016.
- [24] Seong Joon Oh, Bernt Schiele, and Mario Fritz. Towards reverse-engineering black-box neural networks. In *Explainable AI*, volume 11700 of *Lecture Notes in Computer Science*, pages 121–144. Springer, 2019.
- [25] Tribhuvanesh Orekondy, Bernt Schiele, and Mario Fritz. Knock-off nets: Stealing functionality of black-box models. In *CVPR*, pages 4954–4963. Computer Vision Foundation / IEEE, 2019.
- [26] Marek Palatinus, Pavol Rusnak, Aaron Voisine, and Sean Bowe. BIP-39. <https://github.com/bitcoin/bips/blob/master/bip-0039.mediawiki>, 2013.
- [27] Hossein Rezaeighaleh and Cliff C. Zou. New secure approach to backup cryptocurrency wallets. In *GLOBECOM*, pages 1–6. IEEE, 2019.
- [28] Nikola Samardzic, Axel Feldmann, Aleksandar Krastev, Srinivas Devadas, Ronald G. Dreslinski, Christopher Peikert, and Daniel Sánchez. F1: A fast and programmable accelerator for fully homomorphic encryption. In *MICRO*, pages 238–252. ACM, 2021.
- [29] Koen Simoons, Pim Tuyls, and Bart Preneel. Privacy weaknesses in biometric sketches. In *IEEE Symposium on Security and Privacy*, pages 188–203. IEEE Computer Society, 2009.
- [30] Karen Simonyan and Andrew Zisserman. Very deep convolutional networks for large-scale image recognition. In *ICLR*, 2015.
- [31] Florian Tramèr, Fan Zhang, Ari Juels, Michael K. Reiter, and Thomas Ristenpart. Stealing machine learning models via prediction apis. In *USENIX Security Symposium*, pages 601–618. USENIX Association, 2016.
- [32] Erkam Uzun, Carter Yagemann, Simon P. Chung, Vladimir Kolesnikov, and Wenke Lee. Cryptographic key derivation from biometric inferences for remote authentication. In *AsiaCCS*, pages 629–643. ACM, 2021.
- [33] Binghui Wang and Neil Zhenqiang Gong. Stealing hyperparameters in machine learning. In *IEEE Symposium on Security and Privacy*, pages 36–52. IEEE Computer Society, 2018.
- [34] Lukas Zobernig, Steven D. Galbraith, and Giovanni Russello. When are opaque predicates useful? In *TrustCom/BigDataSE*, pages 168–175. IEEE, 2019.